Available online at www.sciencedirect.com
ScienceDirect
Journal of the European Ceramic Society 26 (2006) 3123–3131
www.elsevier.com/locate/jeurceramsoc

# Drying behaviour of droplets of mixed powder suspensions

Jian Wang, Julian R.G. Evans *

*Department of Materials, Queen Mary, University of London, Mile End Road, London E1 4NS, UK*

Received 21 June 2005; received in revised form 12 August 2005; accepted 16 August 2005
Available online 2 November 2005

**Abstract**

Droplets of aqueous multi-component ceramic suspensions were placed on silicone release paper and allowed to dry. The contact angle and height of droplets containing large amounts of dispersant steadily reduced during drying until a minimum value was reached; the contact diameter being almost unchanged during drying. These droplet residues retained a dome shape with uniform compositional distribution of powder. On the other hand, droplets of suspensions containing small additions of dispersant terminated in a 'doughnut' shaped residue sometimes with a central hole and with segregation of powder on the upper surface. For droplets of powder without dispersant, the drying behaviour and compositional distribution varied with the powder characteristics. Two types of particle flow are thought to be responsible for these differences. In general, restricted particle mobility in the droplet produced dome-shaped residues and negligible segregation. This investigation has implications for ink-jet printing of thick-film, combinatorial libraries, and functional gradients.


*Keywords:* Suspensions; Mixing; Drying; Droplets; $Al_2O_3$; $TiO_2$; $ZrO_2$

## 1. Introduction

In general, the drying of ceramic suspensions can be divided into two stages.[1] In the initial constant-rate period, fluid is transported to the external surfaces at a rate that matches evaporation. Then, in the falling-rate period, the fluid can no longer get to the surfaces at this rate and experimentally, there are two falling rate periods. In the first (linear) period, fluid menisci retreat into the body (the funicular state). Moisture migration is controlled by capillary flow. As further evaporation occurs, fluid resides in isolated pockets (the pendular state), marking the transition to a second non-linear falling rate period. The remaining liquid is removed from the body by vapour-phase diffusion.

On the other hand, the drying of drops of liquid deposited on a horizontal non-porous substrate is affected by: (1) the wetting characteristics of the substrate;[2] (2) the temperature and atmospheric conditions;[3] and (3) the properties of the liquid and solids it may contain. Thus, Shannahan and Bourges[3] showed that in a dry environment, a pure water droplet placed on a smooth polymer surface, experienced three stages of drying. First, the contact diameter remained constant whilst both drop height and contact angle decreased. Second, both the drop height and diameter decreased concomitantly while maintaining a small contact angle. Finally, height, diameter and contact angle all decreased sporadically as the droplet volume diminished to zero.

There have been many studies of the drying of unsupported droplets of ceramic slurries, the better to understand spray drying.[4–6] There are studies of the drying of droplets where solutes form a crust[7] and of the surprising shapes that such drops adopt as the crust deforms.[8] More recently, droplet evaporation has attracted popular attention in explaining the ring stains that form when beverage spillages dry.[9] The drying of drops of colloidal suspension is an important step in a diverse range of applications such as protective coatings, fire suppression[10] and ceramic colloidal processing. Here, we explore the drying of droplets of colloidal suspensions of *mixed* oxides, our concern being the formation of individual members of thick film combinatorial libraries prepared by ink-jet printing such that each droplet might have a different composition.[11–13] It is perhaps remarkable that such a formally simple experiment should involve so many complex colloidal and fluid flow processes and we use these processes to interpret the drying of thick-film combinatorial libraries; the drop residue shape that forms and the possible segregation of different powders.

There is general agreement that unlike a sessile drop of pure liquid, for which the contact radius decreases during drying,

* Corresponding author. Tel.: +44 20 7882 5501; fax: +44 20 8981 9804.
*E-mail address:* j.r.g.evans@qmul.ac.uk (J.R.G. Evans).

0955-2219/$ – see front matter © 2005 Elsevier Ltd. All rights reserved.
doi:10.1016/j.jeurceramsoc.2005.08.018

presenting a receding contact angle, the three-phase boundary of a droplet of suspension is pinned by the rapid deposition of particles at the boundary.[14] The pinning is generally attributed to surface irregularities and can be eliminated by using smooth Teflon™ as the substrate.[14] The consequence is that while the radius remains constant, either the drop shape ceases to be a spherical cap, the cap recedes to the centre leaving a foot or the contact angle decreases. In some cases, a series of concentric rings is formed as the droplet dries rather than one peripheral ring.[15]

Guo and Lewis[16] characterized the microstructure of dried films prepared from aqueous $SiO_2$ suspensions stabilized by electrolyte ($NH_4Cl$). Non-uniformities developed in the spatial distribution of colloidal particles and precipitated salt. $SiO_2$ films were cast onto (0 0 1) silicon substrates. The salt concentration decreased substantially from the film edge to its centre as evident in EDS analysis. Such features resulted from capillary induced transport of free colloidal particles and dissolved salt species.

Parisse and Allain[17] demonstrate that a 'foot' becomes fixed around the edge of the droplet where particles build up as drying proceeds. The remaining drop, treated as part of a spherical cap recedes into the centre and they calculate its shape based on the radial flow of liquid to the periphery resulting from the higher relative proportion of liquid–air interface there. For their experiments, the drops were of an aqueous silica colloidal sol containing 24 vol.% solids deposited on cleaned glass. Maenosono et al. reported[18] a system in which two types of particles, CdS and CdSe/CdS(core/shell) were suspended in pyridine and water, respectively. A drop of suspension was placed on a solid substrate and the solvent was allowed to evaporate in a nitrogen atmosphere. A ring-shape multilayer formed at the drop periphery, with the ring width depending on the particle volume fraction. Such lateral transport of carrier liquid has been observed directly by magnetic resonance microscopy during the drying of emulsion paints.[19] This process, modeled by Routh and Russel[20] shows how a front of closely packed particles advances from the drying edge as solvent recedes into the film.

The full story of droplet drying and of the effects reported here, cannot be told until it is recognized that another factor is at play. The splendid observational work presented in a paper by Haw et al.[21] tells us that as the more densely packed particle assembly at the droplet periphery grows, vertical circulation flows are present in the undried central region of the droplet: "aggregates in the cap are seen to continuously circulate in the vertical plane" and so "we can expect *macroscopic* inhomogeneity in the final residue". Later, convection-like cells form in the horizontal plane. The packing of particles in the 'foot' does not become fully dense until the liquid-rich cap has dried. The radial flow of liquid continues to supply the foot to replace the liquid lost there by evaporation. Only when the cap disappears and no replacement is available does the foot become well packed. Very recently, the circulation flows have been analysed by Hu and Larson[22] in terms of the Marangoni stresses that result from surface tension gradients in an evaporating droplet.

In this paper, droplets from various multi-component ceramic colloids were placed on silicone release paper. Their drying behaviour and the compositional distribution in the residues were investigated because of the importance of compositional uniformity of thick-film combinatorial library members. Ink-jet printing provides an opportunity to build and test large numbers of samples for functional properties.[11] The droplet residues require uniform planned composition and optimum shape for measurement.[12] Ink-jet printing is also used as a solid freeforming method for ceramics in which small complex shapes with functional gradients can be downloaded from a computer file by multi-layer addition[23,24] for which compositional control is essential.

## 2. Experimental details

Table 1 describes the materials and lists their sources. The alumina is a fine milled submicron powder that is widely used in industry. The $TiO_2$ is an anatase pigment used in paint formulations. The pure zirconia, selected for compositional analysis using EDS avoids the confounding effect of dopant oxides. Dispex A40 is a solution of an ammonium salt of an acrylic polymer in water widely used to stabilize oxides in aqueous media.

Table 2 gives the composition of ceramic suspensions. After mixing, these were subjected to dispersion using ultrasound (ultrasonic probe model U200S, IKA, Staufen, Germany) pulsed at 0.5 Hz and 75% amplitude for 1 ks. No attempt was made to modify pH, which was between 7 and 8 after ink preparation. The suspensions were deposited using a fine wire at 24 °C and ambient air conditions (31% R.H.). Each drop was approximately 5 μL. The substrate was silicone release paper (Sterling Coated Materials, Cheshire UK) having a surface free energy of 20 mN $m^{-1}$. The drying was observed by optical microscopy and classified. Several examples of drying were imaged as a function of time by a video camera (model 4540, Eastman Kodak Co., San Diego, USA). The contact angle $\theta$, contact diameter $D$, and height of droplets $H$, were computed from the images as illustrated in Fig. 1.

After drying, the residues were removed from the silicone release paper, photographed and the top surfaces, lower surfaces and cross-sections were subjected to EDS analysis as

Table 1
Materials used in ceramic suspensions and their sources

| Material | Supplier | Grade | Purity (%) | Density (kg $m^{-3}$) | Average particle size (μm) |
|---|---|---|---|---|---|
| $Al_2O_3$ | Alcoa, Ludwigshafen, Germany | A16-SG | 99.8 | 3987 | 0.5 |
| $TiO_2$ (Anatase) | Tioxide Europe SA, Calais, France | A-HR | 99.0 | 3850 | 0.15 |
| $ZrO_2$ | Pi-Kem, Shropshire, UK | – | 99.5 | 5750 | 0.9 |
| Dispersant | Allied Colloids Ltd., Bradford, UK | Dispex A40 | – | 1300 | – |

Table 2
The composition of ceramic colloidal suspensions

| Ink I.D. | Planned composition (wt.%) | $Al_2O_3$ powder (wt.%) | $TiO_2$ powder (wt.%) | $ZrO_2$ powder (wt.%) | Dispex A40 (wt.%) | Distilled water (wt.%) |
|---|---|---|---|---|---|---|
| A | $ZrO_2$ 100 | – | – | 38.83 | 1.52 | 59.65 |
| B | $TiO_2$ 100 | – | 29.93 | – | – | 70.07 |
| C | $Al_2O_3$ 100 | 30.46 | – | – | 0.77 | 68.77 |
| D | $Al_2O_3$ 50; $ZrO_2$50 | 17.07 | – | 17.07 | 1.1 | 64.76 |
| E | $Al_2O_3$ 50; $ZrO_2$50 | 17.07 | – | 17.07 | – | 64.76 + 1.1 |
| F | $Al_2O_3$ 50; $ZrO_2$ 50 | 17.07 | – | 17.07 | 10 | 55.86 |
| G | $TiO_2$ 50; $ZrO_2$ 50 | – | 16.9 | 16.9 | 0.66 | 65.54 |
| H | 50 $TiO_2$; 50 $ZrO_2$ | – | 16.9 | 16.9 | – | 65.54 + 0.66 |
| I | 50 $TiO_2$; 50 $ZrO_2$ | – | 16.9 | 16.9 | 10 | 56.2 |
| J | $Al_2O_3$ 25; $TiO_2$ 25; $ZrO_2$ 50 | 8.49 | 8.49 | 16.98 | 0.88 | 65.16 |
| K | $Al_2O_3$ 25; $TiO_2$ 25; $ZrO_2$ 50 | 8.49 | 8.49 | 16.98 | 10 | 56.04 |

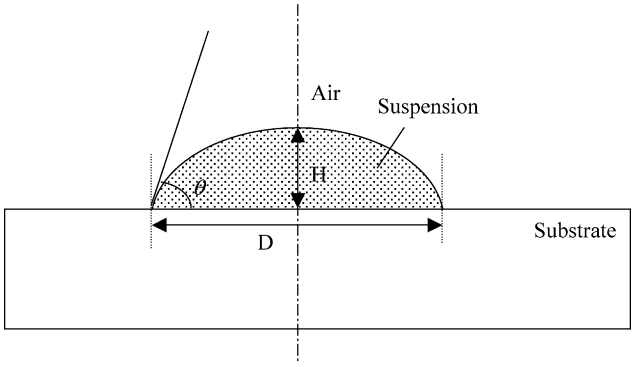


Fig. 1. Schematic representation of a sessile drop of ceramic suspension.

illustrated in Fig. 2 after coating with carbon. The microscope (SEM; Model 6300, JEOL, Tokyo, Japan) was equipped with an EDS system (Model eXL II, Oxford instruments, Bucks, UK). Measurement was taken over an area approximately 150 μm × 150 μm for the upper and lower surfaces and 50 μm × 50 μm for the cross section for a period of 100 s. The conditions were 20 kV acceleration voltage and 15 mm working distance. The data were corrected using INCA software (Oxford Instruments). Cobalt was used as a standard for calibration of the analyzer. The viscosity of ceramic suspensions was measured at 25 °C using a reverse flow U-Tube viscometer following BS 188:1977.

## 3. Results

The ceramic suspensions (Table 2) can be classified in three types based on the amount of dispersant used. Type I consist of mixtures with large (10%) additions of dispersant, (Inks F, I and K). This is far more than that needed to provide stabilization against sedimentation for several hours to allow printing. Type II are mixtures (inks A, C, D, G and J) containing a smaller amount dispersant (∼1 wt.%), though more than enough to preserve stability for the purpose of printing. Type III are mixtures of water and powders without dispersant (Inks B, E and H).

Droplets from type I suspensions present consistent drying behaviour. As shown in Fig. 3a using Ink K as the example, the contact angle and height of droplets steadily reduced until a minimum value was reached. The contact diameter was almost

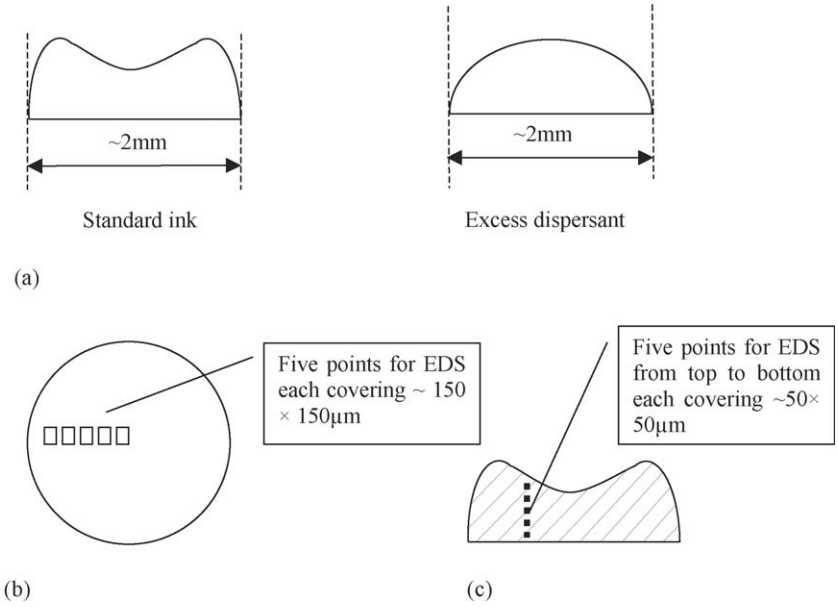


Fig. 2. EDS analysis positions on upper surfaces, lower surface and cross sections.

unchanged during drying. The droplet that began as a spherical cap completed drying still as a dome as shown in Fig. 4a. The residues have uniform planned distribution of powder on both upper and lower surfaces and on cross sections as analyzed by EDS and given in Table 3 rows 3, 6 and 8. Such droplets form ideal combinatorial library members because their shape is suited to testing by electrical or optical probes and composition is consistent.

Droplets of type II suspensions (∼1 wt.% dispersant) had a quite different drying behaviour. Using Ink J as the example (Fig. 3b), in the first stage, up to 0.9 ks, the contact angle and height of droplets consistently decreased. In the second stage, at constant contact angle, the height of droplets decreased. In the last stage, both the apparent height of droplets and the contact angle were unchanged but the silhouette imaged against back-illumination does not disclose the pronounced collapse of the central region. The bulk of the ceramic powder, now situated at the rim, subsequently dried. Type II residue therefore ended as a 'doughnut' shape sometimes with a hole in the centre as shown in Fig. 4b.

When EDS analysis was performed on these residues, the lower surface and cross-sections agreed with the planned composition but segregation of powders occurred on the upper surface (Table 3, rows 1, 4 and 7). This variation is to a depth of about 10 μm and decreases both towards the centre and outside of the drop residue. Cracking of the residue could also be found sometimes. These are not suitable for combinatorial work because the shape does not allow access by measurement probes and the composition varies on the upper surface.

For Type III suspensions to which no dispersant was added, the drying patterns depended on the powder. The drying of droplets from Ink E ($Al_2O_3$–$ZrO_2$ system) was similar to Type I suspensions that contained excess dispersant. Both the contact angle and height of droplets consistently reduced until a minimum value was reached. The contact diameter was almost unchanged during drying. The residue also retained a dome and had uniform planned powder distribution as did the residues from the droplets of type I suspensions as shown in Table 3, rows 2. For other type III suspensions, (Ink B; single component $TiO_2$ ink) and H ($TiO_2$–$ZrO_2$ system without dispersant), the drying was similar to type II inks that contained around 1% dispersant, experiencing three stages as described above. The EDS result of the residue of droplets from Ink H (Table 3, rows 5) shows non-uniform compositional distribution. The resulting residue also had a 'doughnut' shape, as did the type II inks. The residue of droplets from Ink H is shown in Fig. 4c.

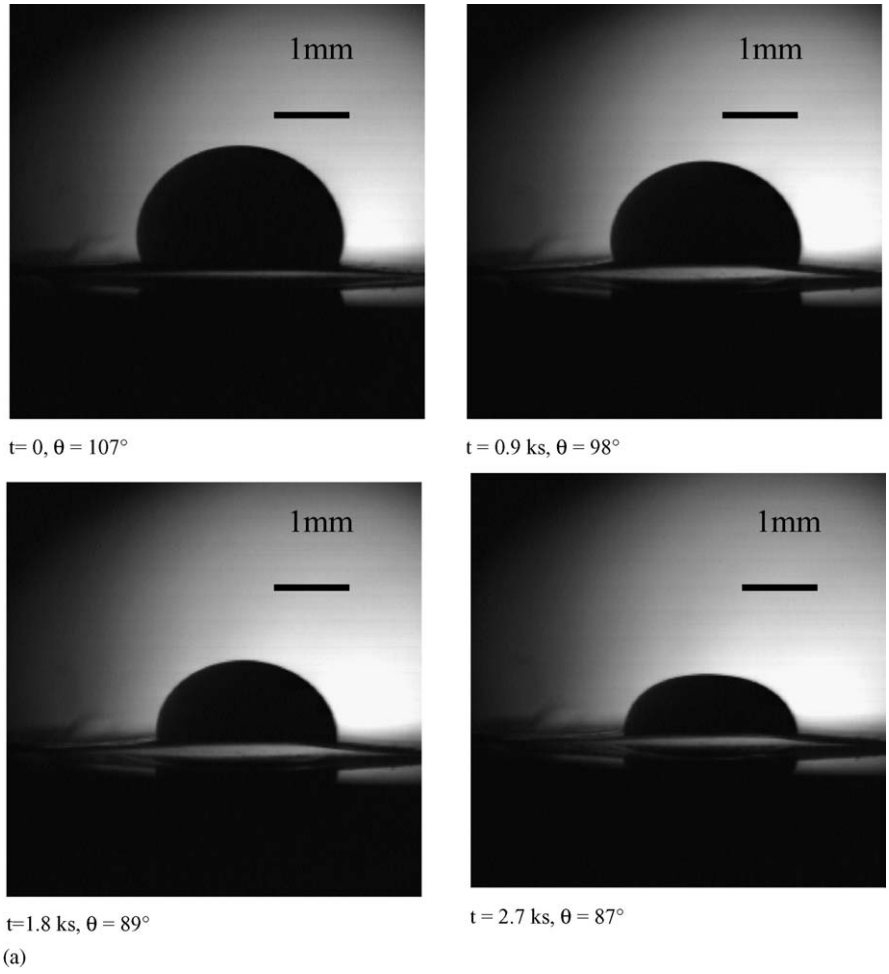


Fig. 3. The drying of a droplet of ceramic suspension containing: (a) excess amount of dispersant deposited on silicone release paper. (Ink K) at $t = 0$, 0.9, 1.8 and 2.7 ks: (b) approximately 1 wt.% dispersant deposited on silicone release paper (Ink J) at $t = 0$, 0.6, 1.2 and 2.1 ks.

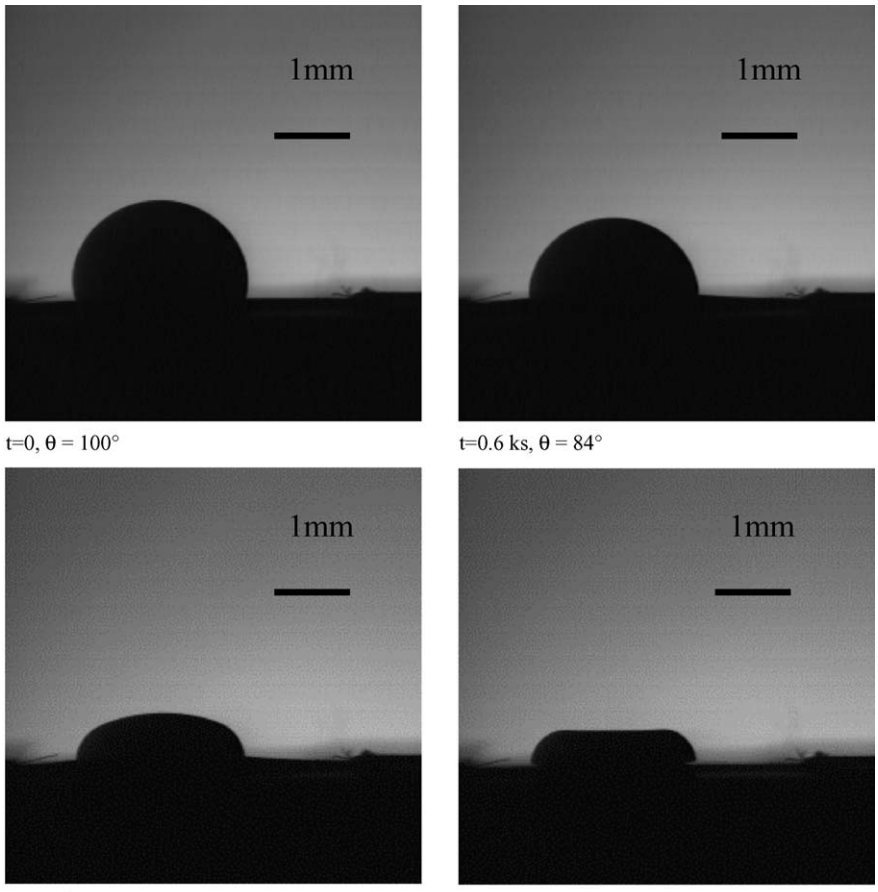


Fig. 3. (*Continued*).

Table 3
EDS analysis of droplet residues of multi-component ceramic colloids

| Ink I.D. | Dispex (wt.%) | Planned composition (wt.%) | EDS analysis (wt.%)[a] | | |
|---|---|---|---|---|---|
| | | | Top surface | Lower surface | Cross section |
| D | 1.1 | $Al_2O_3$ 50 | 27 ± 9 | 48 ± 1 | 48 ± 2 |
| | | $ZrO_2$ 50 | 73 ± 9 | 52 ± 1 | 52 ± 2 |
| E | 0 | $Al_2O_3$ 50 | 49 ± 1 | 49 ± 1 | 48 ± 1 |
| | | $ZrO_2$ 50 | 51 ± 1 | 51 ± 1 | 52 ± 1 |
| F | 10 | $Al_2O_3$ 50 | 50 ± 3 | 52 ± 1 | 51 ± 2 |
| | | $ZrO_2$ 50 | 50 ± 3 | 48 ± 1 | 49 ± 2 |
| G | 0.66 | $TiO_2$ 50 | 10 ± 21 | 48 ± 1 | 47 ± 1 |
| | | $ZrO_2$ 50 | 90 ± 21 | 52 ± 1 | 53 ± 1 |
| H | 0 | $TiO_2$ 50 | 58 ± 11 | 33 ± 7 | 29±26 |
| | | $ZrO_2$ 50 | 42 ± 11 | 67 ± 7 | 71±26 |
| I | 10 | $TiO_2$ 50 | 50 ± 4 | 46 ± 1 | 47 ± 2 |
| | | $ZrO_2$ 50 | 50 ± 4 | 54 ± 1 | 53 ± 2 |
| J | 0.88 | $Al_2O_3$ 25 | 12 ± 11 | 26 ± 1 | 25 ± 2 |
| | | $TiO_2$ 25 | 9 ± 12 | 24 ± 0 | 24 ± 2 |
| | | $ZrO_2$ 50 | 79 ± 22 | 50 ± 1 | 51 ± 3 |
| K | 10 | $Al_2O_3$ 25 | 25 ± 1 | 26 ± 0 | 24 ± 1 |
| | | $TiO_2$ 25 | 25 ± 1 | 23 ± 0 | 24 ± 1 |
| | | $ZrO_2$ 50 | 50 ± 1 | 51 ± 0 | 52 ± 1 |

[a] Average for five arrays at different positions shown in Fig. 2 with 95% confidence limits.

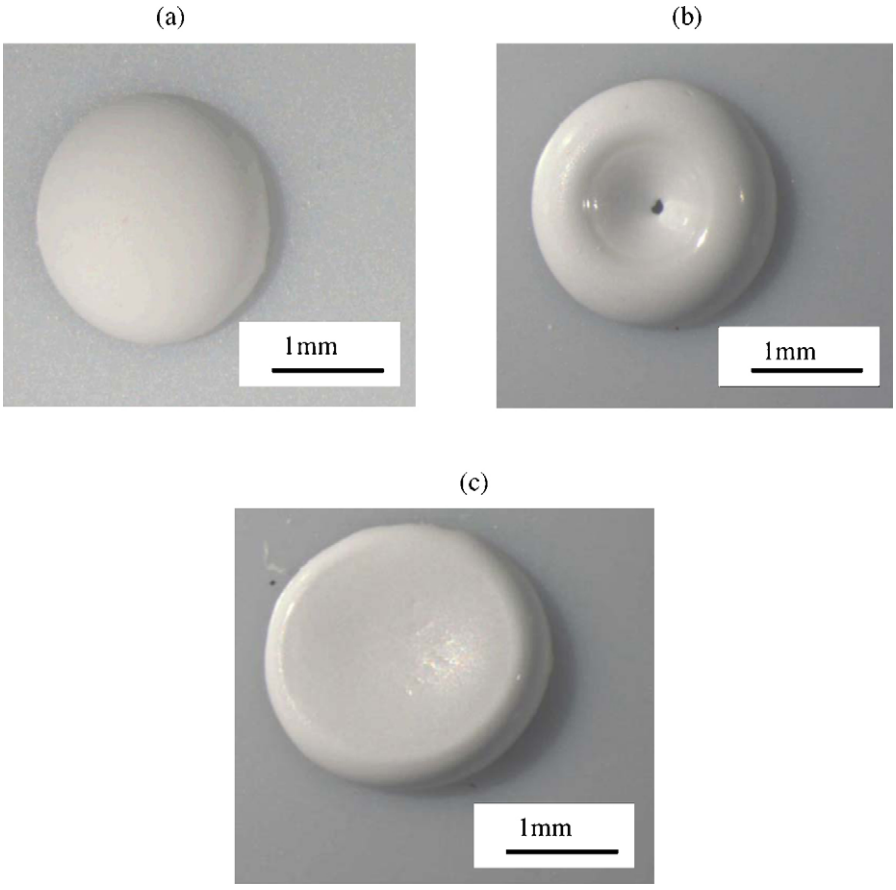


Fig. 4. The shape of droplet residues: (a) colloidal suspension containing excess amount of dispersant (Ink K); (b) colloidal suspension containing around 1 wt.% dispersant (Ink J); and (c) suspension containing no dispersant (Ink H).

## 4. Discussion

Many observers[19–21] point out that the relative proportion of liquid–air interface is larger near the edge and this provides models of drying.[14,15,19,20,25] Since the ratio of liquid–air interface relative to the underlying liquid is larger near the drop periphery a large amount of solvent is lost in this area and if the droplet footprint is unchanged, finite flow in the radial direction of the footprint occurs during drying. Some[19,20] consider that the evaporation rate can be taken as constant across the droplet surface, while others[9,14] attribute a higher evaporation rate to the droplet edge in static air because of the lower vapour pressure over the surrounding substrate. Most observers see the formation of a 'foot' consisting of a pile-up of particles at the droplet periphery which starts to form in the early stages of drying and continues to grow.[14,15,17,19,21] When the droplet was mounted on a pedestal and surrounded by a water bath so that there is a uniform partial pressure of vapour over the whole surface of the droplet, a peripheral deposit still formed.[14] Interestingly, when the drop was covered with a chamber with a small hole over the centre of the evaporating drop, a peripheral foot of solids did not form and a uniform deposit resulted.

A rather simplified geometry illustrates the strong variation in surface area to underlying volume but without accounting for the flow paths. Consider a hemisphere of radius, $r$ as shown in Fig. 5a sliced parallel to the equatorial plane. The surface area of a slice, $A$, is dependant only on the thickness;

$$A = 2\pi r(r - h), \tag{1}$$

The volume of a slice that has a base on the equator is:

$$V_s = \frac{\pi}{3}(2r^3 - 3rh^2 + h^3) \tag{2}$$

The volume of the cylinder inside the slice is:

$$V_c = \pi x^2(r - h), \tag{3}$$

but since $x^2 = 2rh - h^2$ ($x$ is shown in Fig. 5a),

$$V_c = \pi(2r^2h - 3rh^2 + h^3) \tag{4}$$

the volume of the rim is $V_R = V_s - V_c$ and from Eq. (2) and (3) is:

$$V_R = \frac{\pi}{3}(2r^3 + 6rh^2 - 6r^2h - 2h^3) \tag{5}$$

from Eqs. (1) and (5), the ratio of surface area $A$ to volume of rim $V_R$ is:

$$\frac{A}{V_R} = \frac{3r}{(r - h)^2}, \tag{6}$$

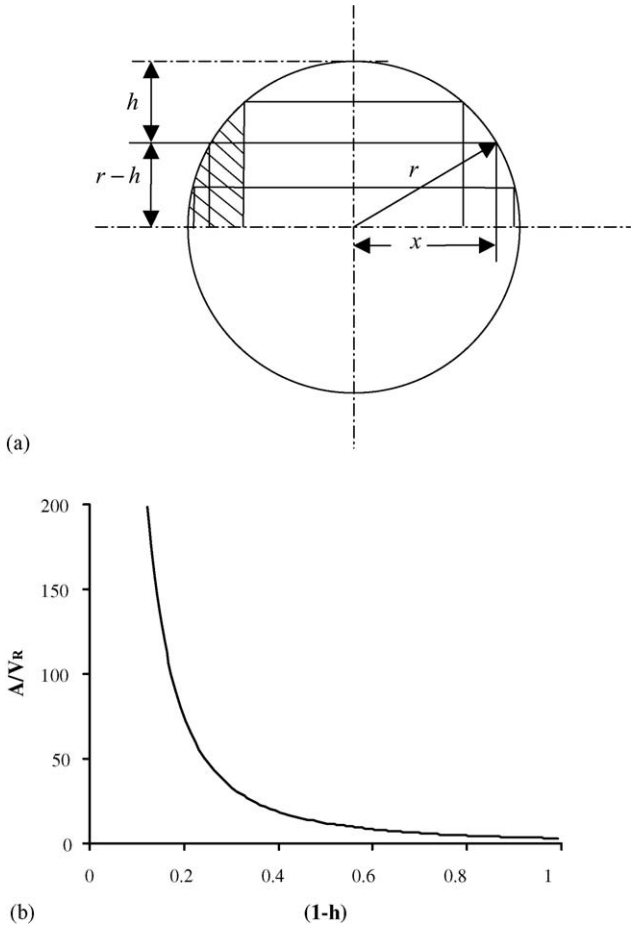


Fig. 5. (a) Model of a hemispherical cap showing droplet edge as shaded and (b) surface area/volume ratio as a function of $(1-h)$ for $r=1$.

Eq. (6) is plotted for $r=1$ in Fig. 5b showing how the ratio of surface area to volume increases towards the periphery of drop for the case of a 90° contact angle. Obviously a ratio of $3/r$ is obtained for the hemisphere at $h=0$. This does not address the more complex flow paths that occur during drying but does show that a strong component of flow must occur in the radial direction of the droplet footprint even if drying is uniform over the liquid surface.

Droplets placed on silicone release paper start with a contact angle greater than 90° and, as evaporation proceeds, the contact angle reduces to 90° (hemisphere), as the edge region dries first. The droplet curve is no longer spherical because the contact diameter stays the same. Neither is the curvature continuous because solids pile up at the periphery. The final droplet shape therefore depends on the extent to which powder participates in this flow.

We propose that the geometry and compositional distribution of residues of droplets are both related to the movement of particles during drying but to different types of flow. Thus, non-uniform composition and droplet residue shape are related to the mobility of particles in the drop. The question is, why, when the edge dried first in all ceramic ink droplets, do droplets of Type I suspension retain a dome shape and do not show segregation in the residue whereas droplets of type II suspension end as a

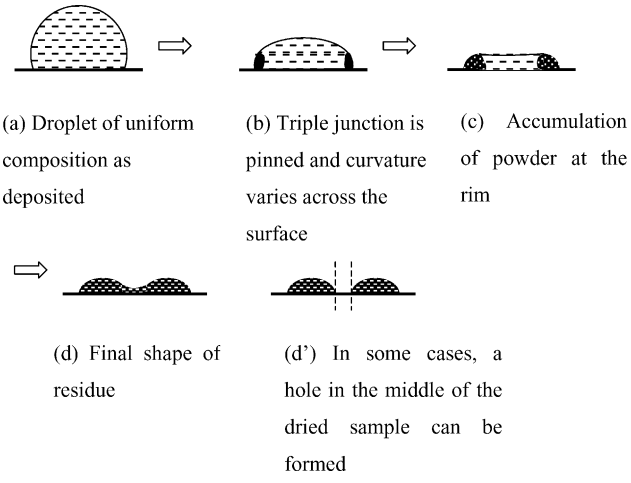


Fig. 6. Schematic diagram of the drying process of droplets from suspensions containing ~1 wt.% dispersant. Recirculation flows are present in the dashed region.

'doughnut' shape with segregation of powders of the residues? Two possible reasons stand out: (1) flocculation induced by entanglement of excess dispersant molecules inhibits particles from participating in flow during drying and (2) increased liquid viscosity due to excess dispersant prevents movement of particles in the suspension. There is a striking parallel with the morphological development of residues from spherical spray dried ceramic agglomerates; droplets from well-dispersed slurries in which particles retain mobility during drying, form irregular shaped agglomerates with a central hole. Suspensions with a tendency to flocculate, form dense spherical agglomerates.[5]

Careful observation of Type II droplets during drying shows that early in the process, a high packing density of powder builds up at the periphery of the drop. The three dimensional network of particles that forms here is well known (vide supra). The rim of the drop accumulates powder and becomes larger forming a solid-like ring that can be observed on the drop periphery as a discontinuity of curvature seen in Fig. 4b and shown schematically in Fig. 6. Eventually a 'doughnut' shape forms in which the centre is depleted in powder, sometimes leaving a hole. Clearly particle motion to the periphery accompanies radial liquid flow in the case of these drops. This flow explains the droplet shape but not the segregation effects.

The second type of flow is the recirculation currents observed by Haw et al.[21] and modeled in terms of Marangoni flows by Hu and Larson.[22] This liquid region has the shape delineated by the dashed region in Fig. 6 and within it circulation flows persist, driven by Marangoni stresses that result from temperature gradients and in turn, surface energy gradients, due to evaporation. These dramatic recirculation currents can be seen in an optical microscope fitted with oblique illumination.

We suggest that as some particles become immobilized in the peripheral 'foot' the recirculation region contains an excess of the particles that are best dispersed and therefore least able to join the 'foot' which they do by a flocculation mechanism. The upper surface within the peripheral foot is thus the last to 'solidify' and this is precisely the region where segregation effects are observed. In all our experiments it is the powder

Table 4
Viscosities of suspensions

| Ink I.D. | Dispersant in the suspension (wt.%) | Kinematic viscosity ($mm^2 s^{-1}$) |
|---|---|---|
| $Al_2O_3$–$ZrO_2$ system | | |
| D | 1.1 | 1.47 |
| F | 10 | 3.66 |
| $TiO_2$–$ZrO_2$ system | | |
| G | 0.66 | 1.38 |
| I | 10 | 11.42 |

that is better dispersed that resides in excess on this part of the upper surface. Table 4 indicates that the bulk viscosity if type I inks is indeed higher than that of type II but this does not fully disclose the entanglement effects of excess dispersant which may also reduce particle mobility. It may also be possible for fine powders to filter through denser packed regions of coarse particles to the surface as radial liquid flow occurs but the preferred segregation of coarse particles suggests this is a secondary effect.

It is important to note that the segregation of powders occurring on the upper surface of the residues (Table 3, rows 1, 4 and 7) is not what would be expected from preferential sedimentation. The $ZrO_2$ has the highest density and largest average particle size, followed by $Al_2O_3$, and $TiO_2$ powder which has the lowest density and average particle size. In the $ZrO_2$–$TiO_2$ system, $ZrO_2$–$Al_2O_3$ system and $ZrO_2$–$Al_2O_3$–$TiO_2$ system, $ZrO_2$ should preferentially sediment. The results indicate that $ZrO_2$ is much richer than planned on the upper surface of residues for all systems (Table 3, row 1, 4 and 7).

For Type III suspensions, which are dispersant-free, both behaviours, as well as preferential sedimentation, are observed during drying depending on the powder. Taking the $Al_2O_3$–$ZrO_2$ system (suspension E), there was a noticeable, but not measured, increase in viscosity without dispersant. This is typical of flocculated suspensions.[26] The spherical cap shape and homogenous mixture end as a dome with uniform planned distribution of powder (Table 3, rows 2) and it seems reasonable to speculate that this is because a three dimensional flocculated network prevents particles from participating the liquid flow to the droplet periphery. Thus, limited particle motion in the drop prevents particles taking part in both types of flow.

On the other hand, suspension H ($TiO_2$–$ZrO_2$ system without dispersant) does show evidence of preferential sedimentation. $TiO_2$ is a fine powder that disperses well in water even without addition of dispersant. $ZrO_2$ is a comparatively coarse powder as deduced from SEM images. These droplets ended as a much flatter doughnut shape as shown in Fig. 4c. After drying, $TiO_2$ was richer on the upper surface while $ZrO_2$ powder was preferentially sedimented on the lower surface.

## 5. Conclusions

An initial attempt is made to account for the different profiles that result from the drying of multi-component colloidal ceramic suspensions and the associated compositional non-uniformities that develop. By varying the amount of dispersant, two distinct drying regimes are obtained giving distinct droplet profiles after drying and these correlate with segregation of powder or its absence on the upper surface. The results are material to the thick-film ink-jet printing of ceramic combinatorial libraries in which compositional homogeneity is sought.

For droplets of suspension in which there is limited particle mobility either due to excessive loadings of dispersant or because of absence of dispersant, the contact angle and height of droplets consistently reduced until a minimum value was reached. The contact diameter was almost unchanged during drying. Droplet residues retained a dome shape with uniform planned distribution of powder. These suspensions are ideal for combinatorial ink-jet printing even though they might not be better dispersed.

Droplets of suspension in which particles are mobile, such as those containing around 1 wt.% dispersant or fine powder that disperse well in water without the addition of dispersant, a ‘doughnut’ shape of residue sometimes with a central hole resulted. Segregation of powders occurred in these drops and it was contrary to that expected from preferential sedimentation. We attribute it to recirculation flows in the fluid part of the drop, which retains the better dispersed powder to the end of drying.

## References


1. Lewis, J. A., Colloidal processing of ceramics. *J. Am. Ceram. Soc.*, 2000, **83**(10), 2341–2359.
2. Lau, W. W. Y. and Burns, C. M., Kinetics of spreading—polystyrene melts on plane glass surfaces. *J. Colloid Interface Sci.*, 1973, **45**(2), 295–302.
3. Shanahan, M. E. R. and Bourges, C., Effects of evaporation on contact angles on polymer surfaces. *Int. J. Adhes. Adhes.*, 1994, **14**(3), 201–205.
4. Cheong, H. W., Jeffreys, G. V. and Mumford, C. J., A receding interface model for the drying of slurry droplets. *AICHE J.*, 1986, **32**(8), 1334–1346.
5. Fair, G. E. and Lange, F. F., Effect of interparticle potential on forming solid, spherical agglomerates during drying. *J. Am. Ceram. Soc.*, 2004, **87**(1), 4–9.
6. Elperin, T. and Krasovitov, B., Evaporation of liquid droplets containing small solid particles. *Int. J. Heat Mass Transf.*, 1995, **38**(12), 2259–2267.
7. Audu, T. O. K. and Jeffreys, G. V., The drying of drops of particulate slurries. *Trans. Instn. Chem. Engrs.*, 1975, **53**(3), 165–172.
8. Pauchard, L. and Allain, C., Stable and unstable surface evolution during the drying of a polymer solution drop. *Phys. Rev. E.*, 2003, **68**(5), 052801-1-4.
9. Deegan, R. D., Bakajin, O., Dupont, T. F., Huber, G., Nagel, S. R. and Witten, T. A., Capillary flow as the cause of ring stains from dried liquid drops. *Nature*, 1997, **389**(6653), 827–829.
10. Chandra, S., di Marzo, M., Qiao, Y. M. and Tartarini, P., Effect of liquid-solid contact angle on droplet evaporation. *Fire Saf. J.*, 1996, **27**(2), 141–158.
11. Evans, J. R. G., Edirisinghe, M. J., Coveney, P. V. and Eames, J., Combinatorial searches of inorganic materials using the ink-jet printer: science, philosophy and technology. *J. Eur. Ceram. Soc.*, 2001, **21**(13), 2291–2299.
12. Wang, J., Mohebi, M. M. and Evans, J. R. G., Two methods to generate multiple compositions in combinatorial ink-jet printing of ceramics. *Macromol. Rapid Commun.*, 2005, **26**(4), 304–309.
13. Wang, J. and Evans, J. R. G., London University Search Instrument: A combinatorial robot for high-throughput methods in ceramic science. *J. Comb. Chem.* 2005, **7**, 665–672.

14. Deegan, R. D., Bakajin, O., Dupont, T. F., Huber, G., Nagel, S. R. and Witten, T. A., Contact line deposits in an evaporating drop. *Phys. Rev. E.*, 2000, **62**(1), 756–765.
15. Adachi, E., Dimitrov, A. S. and Nagayama, K., Stripe patterns formed on a glass surface during droplet evaporation. *Langmuir*, 1995, **11**(4), 1057–1060.
16. Guo, J. J. and Lewis, J. A., Aggregation effects on the compressive flow properties and drying behavior of colloidal silica suspensions. *J. Am. Ceram. Soc.*, 1999, **82**(9), 2345–2358.
17. Parisse, F. and Allain, C., Drying of colloidal suspension droplets: Experimental study and profile renormalization. *Langmuir*, 1997, **13**(14), 3598–3602.
18. Maenosono, S., Dushkin, C. D., Saita, S. and Yamaguchi, Y., Growth of a semiconductor nanoparticle ring during the drying of a suspension droplet. *Langmuir*, 1999, **15**(4), 957–965.
19. Ciampi, E., Goerke, U., Keddie, J. L. and McDonald, P. J., Lateral transport of water during drying of alkyd emulsions. *Langmuir*, 2000, **16**(3), 1057–1065.
20. Routh, A. F. and Russel, W. B., Horizontal drying fronts during solvent evaporation from latex films. *AICHE J.*, 1998, **44**(9), 2088–2098.
21. Haw, M. D., Gillie, M. and Poon, W. C. K., Effects of phase behaviour on the drying of colloidal suspensions. *Langmuir*, 2002, **18**(5), 1626–1633.
22. Hu, H. and Larson, R. G., Analysis of the effects of Marangoni stresses on the microflow in an evaporating sessile droplet. *Langmuir*, 2005, **21**(9), 3972–3980.
23. Mott, M. and Evans, J. R. G., Zirconia/alumina functionally graded material made by ceramic ink jet printing. *Mater. Sci. Eng. A-Struct. Mater. Prop. Microstruct. Process.*, 1999, **271**(1–2), 344–352.
24. Mohebi, M. M. and Evans, J. R. G., A drop-on-demand ink-jet printer for combinatorial libraries and functionally graded ceramics. *J. Comb. Chem.*, 2002, **4**(4), 267–274.
25. Parisse, F. and Allain, C., Shape changes of colloidal suspension droplets during drying. *J. Phys. II France*, 1996, **6**(7), 1111–1119.
26. Luther, E. P., Yanez, J. A., Franks, G. V., Lange, F. F. and Pearson, D. S., Effect of ammonium citrate of the rheology and particle packing of alumina slurries. *J. Am. Ceram. Soc.*, 1995, **78**(6), 1495–1500.